iScience

CellPress
OPEN ACCESS

Article

Differential N-terminal processing of beta and gamma actin

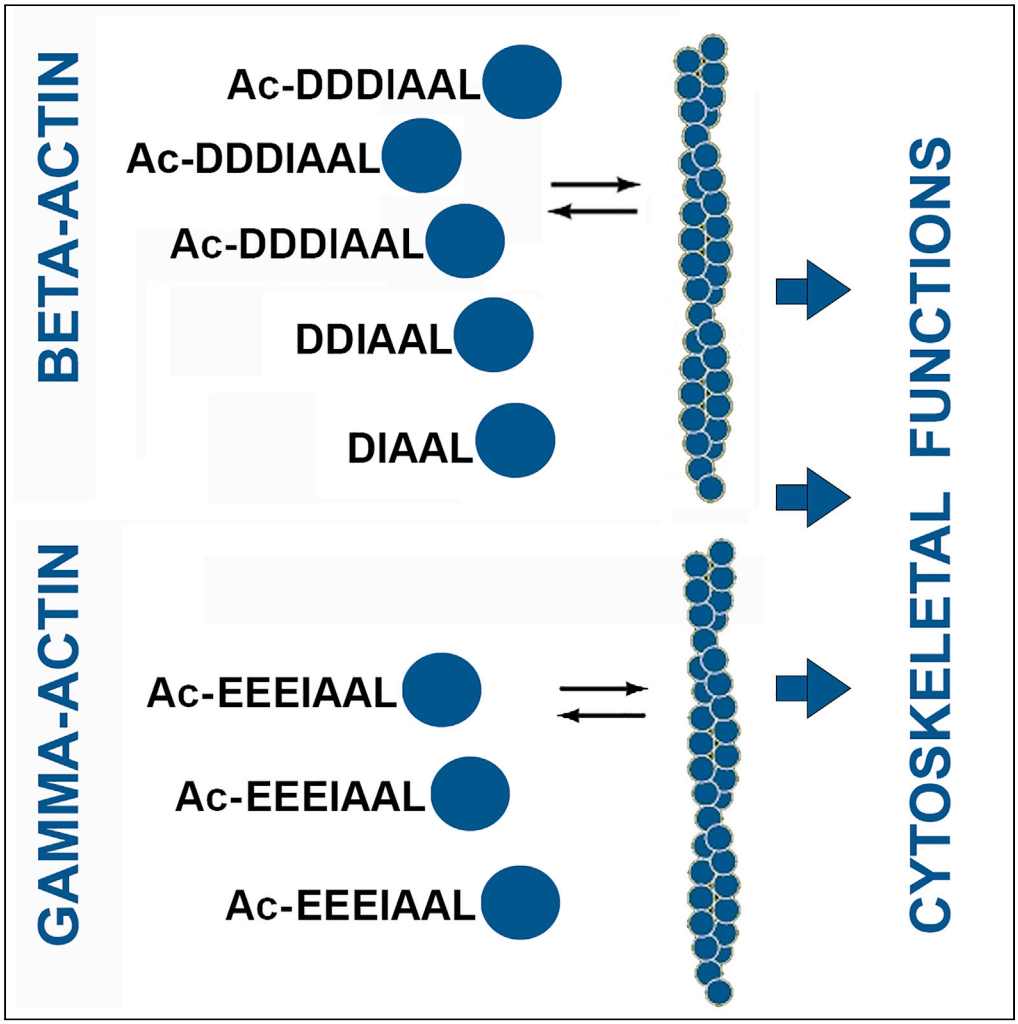

Li Chen, Pavan Vedula, Hsin Yao Tang, Dawei W. Dong, Anna S. Kashina

akashina@upenn.edu

Highlights

Intracellular beta actin is specifically processed by removal of N-terminal residues

N-terminally processed beta actin is found in both F- and G-actin pool

Deletion of N-aminopeptidases affects beta actin, cytoskeleton, and cell motility

Chen et al., iScience *25*, 105186
October 21, 2022
https://doi.org/10.1016/j.isci.2022.105186

iScience

CellPress
OPEN ACCESS

Article

Differential N-terminal processing of beta and gamma actin

Li Chen,[1] Pavan Vedula,[1] Hsin Yao Tang,[2] Dawei W. Dong,[1] and Anna S. Kashina[1,3,*]

SUMMARY

Cytoplasmic beta- and gamma-actin are ubiquitously expressed in every eukaryotic cell. They are encoded by different genes, but their amino acid sequences differ only by four conservative substitutions at the N-termini, making it difficult to dissect their individual regulation. Here, we analyzed actin from cultured cells and tissues by mass spectrometry and found that beta, unlike gamma actin, undergoes sequential removal of N-terminal Asp residues, leading to truncated actin species found in both F- and G-actin preparations. This processing affects up to ~3% of beta actin in different cell types. We used CRISPR/Cas-9 in cultured cells to delete two candidate enzymes capable of mediating this type of processing. This deletion abolishes most of the beta actin N-terminal processing and results in changes in F-actin levels, cell spreading, filopodia formation, and cell migration. Our results demonstrate previously unknown isoform-specific actin regulation that can potentially affect actin functions in cells.

INTRODUCTION

Actin is one of the most essential and abundant intracellular proteins, playing an essential physiological role as the major constituent of the actin cytoskeleton. In mammals, actin family is represented by six highly similar proteins, four that are prevalent in different types of muscle, and two non-muscle actins, beta- and gamma cytoplasmic actin (Bunnell and Ervasti, 2010; Vedula and Kashina, 2018).

Beta- and gamma-actin are nearly identical at the amino acid level but are encoded by different genes that are ubiquitously expressed in every mammalian cell (Bunnell and Ervasti, 2011). Their amino acid sequences differ only by four conservative substitutions at the N-terminus (Vandekerckhove and Weber, 1978a, 1978b, 1978c, 1978d). At the gene level, their functions in cell migration and organism's survival dramatically differ: Beta actin's knockout in mice results in early embryonic lethality and severe impairments of fibroblasts' ability to migrate (Bunnell et al., 2011), while gamma actin's knockout leads to much milder phenotypes (Bunnell and Ervasti, 2010). Our recent work showed that this difference is defined by their nucleotide, rather than amino acid sequence (Vedula et al., 2017). Moreover, we find that the differential effects of beta and gamma actin on cell migration are defined by their nucleotide coding sequence-dependent differences in actin translation elongation rates (Vedula et al., 2021).

Actins *in vivo* undergo N-terminal processing, in which the N-terminal Met is acetylated and removed by a specialized aminopeptidase (Sheff and Rubenstein, 1992), and the second residue – Asp in beta actin and Glu in gamma actin – is post-translationally acetylated (Rubenstein and Martin, 1983). Muscle actins undergo similar processing, even though differences in their N-termini account for slightly different steps preceding acetylation in muscle and non-muscle cells (Solomon and Rubenstein, 1985). Overall, >90% of intracellular actin is acetylated in steady state, and this acetylation facilitates actin's cellular functions (Drazic et al., 2018).

Actin undergoes multiple posttranslational modifications (PTM) (Terman and Kashina, 2013; MacTaggart and Kashina, 2021), however most of these modifications are believed to uniformly affect all actin isoforms, and any examples to the contrary are very difficult to parse out because of the near-identity of actin amino acid sequences and their coexistence in the same cells. One known exception constitutes N-terminal arginylation, which targets the only sequence sufficiently different between non-muscle actins to be detectable by the currently available methods. Earlier studies from our group found that beta, but not gamma actin undergoes N-terminal arginylation on Asp 3, presumably exposed after a previously unknown N-terminal

[1]Department of Biomedical Sciences, University of Pennsylvania School of Veterinary Medicine, Philadelphia, PA 19104, USA

[2]The Wistar Institute, Philadelphia, PA 19104, USA

[3]Lead contact

*Correspondence: akashina@upenn.edu

https://doi.org/10.1016/j.isci.2022.105186

processing step involving removal of the second Asp (Karakozova et al., 2006). Such N-terminal beta actin arginylation affects less than 1% of the total intracellular beta actin pool (Chen and Kashina, 2019), making it extremely difficult to detect. Our work suggest that selective arginylation of beta, but not gamma, actin is defined by their nucleotide coding sequence (Zhang et al., 2010), likely linked to their different translation elongation rates (Vedula et al., 2021), and that this arginylation is essential for cell migration (Karakozova et al., 2006). However, processing steps leading to beta actin's arginylation on Asp 3 have never been described.

Here, we analyzed beta and gamma cytoplasmic actin N-termini *in vivo* and found that beta actin undergoes sequential removal of N-terminal Asp residues, resulting in intracellular actin species lacking one, two, or three Asp from the N-terminus. In contrast, gamma actin does not appear to undergo such processing, and only the N-termini containing Met, or acetylated Glu after Met removal, can be seen. Overall, this processing affects ~1–3% of the total beta actin pool in different cell types. We identified two candidate enzymes, N-terminal Asp and Glu aminopeptidases (DNPEP and ENPEP), and deleted them in human HAP1 cells to assess their role in beta actin processing and the basic properties of the actin cytoskeleton-dependent intracellular processes. We find that while deletion of *DNPEP* does not strongly affect removal of beta actin's N-terminal Asp, *ENPEP* deletion has a much more pronounced effect, and the double knockout leads to nearly complete abolishment of this processing. Although these data suggest that additional, as yet unidentified, enzyme(s) could also mediate this processing and are likely employed in the absence of DNPEP and ENPEP, these two enzymes are likely players in actin N-terminal Asp removal. *DNPEP* and *ENPEP* knockout cells display differences in F-actin levels, cell spreading, filopodia formation, and cell migration, and these effects differ and only partially overlap for DNPEP and ENPEP, suggesting that their knockout phenotypes are only partially actin-related. Although DNPEP and ENPEP are general specificity enzymes that likely affect a number of intracellular targets in addition to actin, this result points to a possibility that the beta actin processing mediated by these enzymes may be physiologically important for beta actin function. *In vitro* experiments with N-terminal beta and gamma actin derived peptides show that ENPEP is capable of targeting both unprocessed beta- and gamma-actin N-termini after Met removal, but neither ENPEP or DNPEP can target the peptides containing N-terminally acetylated Asp or Glu, suggesting that *in vivo* targeting of this processing to beta actin requires additional recognition mechanisms, and that this processing likely occurs prior to actin acetylation. We propose that selective N-terminal processing of beta actin by sequential removal of Asp contributes to differentiating the functions of non-muscle actin isoforms *in vivo*.

RESULTS

Beta and gamma actin are differentially N-terminally processed *in vivo*

To analyze the processing of the actin's N-termini in non-muscle cells, we performed mass spectrometry of total intracellular actin from mouse embryonic fibroblasts (MEF) cell, a commonly used non-muscle migratory cell type that expresses approximately equal levels of beta and gamma cytoplasmic actin.

To capture an enriched fraction of total actin without any bias in purification steps, we fractionated total cell lysates on SDS page and broadly excised a prominent protein band in the ~43 kDa range corresponding to the actin's molecular weight (Figure S1). We then performed in-gel digestion of this band by trypsin and analyzed it by LC-MS/MS. To ensure identification of the processed actin N-termini, we performed searches under semi-tryptic conditions (in which the program considers that a peptide may have been generated by tryptic cleavage on one end, and non-tryptic processing on the other end), since fully tryptic search can only identify unprocessed N-terminal peptides.

This analysis revealed a repertoire of N-terminal peptides derived from both beta and gamma actin (Figure 1A, left panels). As previously shown, the majority of these peptides represented N-terminal acetylation on Asp 2 or Glu 2 in beta and gamma actin, respectively (Figure 1A, top left). A small fraction of the peptides was unprocessed, containing N-terminal initiator Met. To estimate the relative abundance of these peptides we calculated the fraction of each peptide's intensity to the sum of intensities of all the N-terminal peptides for each actin isoform (see Table S2 for raw intensity data). Although not fully quantitative, because of different chemical properties and ionization of different peptides during mass spectrometry, these estimations enabled us to plot the fraction of each modified peptide compare to the total (Figure 1A). Curiously, the fraction of Met containing peptides was somewhat higher in gamma actin (~3%) compared to beta actin (~1%) (Figure 1A, top left). This suggests that the enzyme(s) mediating this removal have a

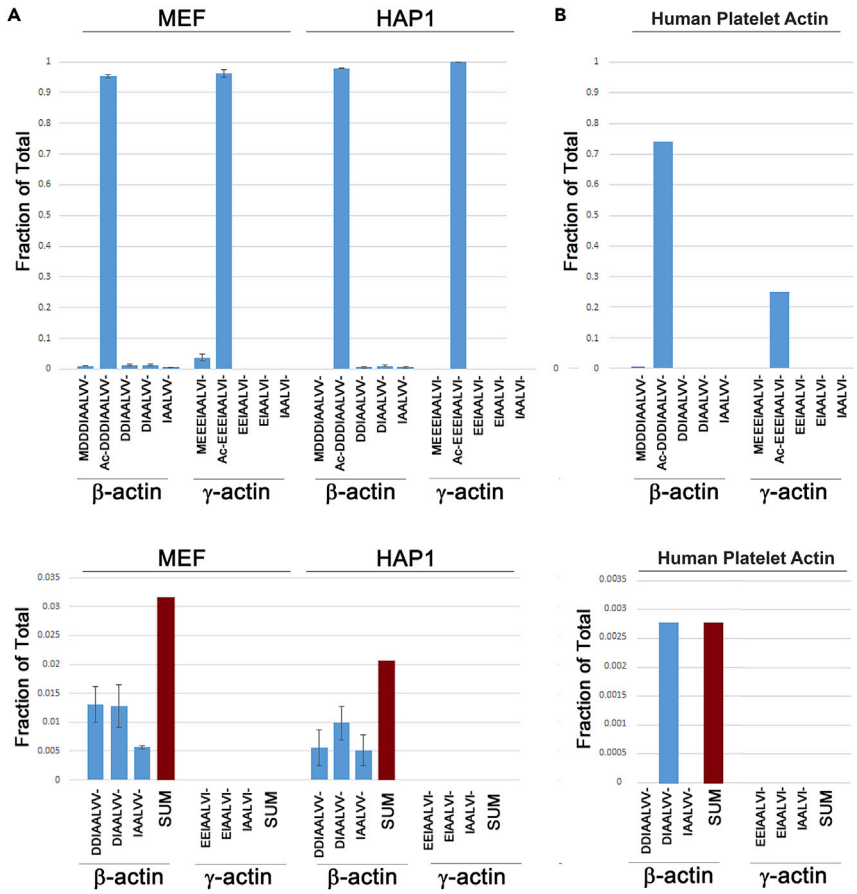

Figure 1. Beta and gamma actin are differentially N-terminally processed in mammalian cells

(A) Mass spectrometry quantification of the N-terminal beta- and gamma-actin peptides in mouse embryonic fibroblasts (MEF) and human HAP1 cells, quantified as the ratio of intensities for each peptide versus the total sum of intensities for the entire set of N-terminal peptides identified for each actin isoform (fraction of the total). N-terminal sequence of each peptide for each isoform is indicated on the X axis. Upper panel, the entire repertoire of N-terminal peptides found in cells. Lower panel, expanded view of the peptides generated by sequential removal of N-terminal Asp residues. Error bars represent SEM, n = 3; see Table S4 for the actual values.

(B) Mass spectrometry detection of N-terminal actin peptides in purified human platelet actin. Results from a single experiment are shown. See Table S2 for the raw intensity values.

slight preference for beta actin, or that gamma actin after Met removal, unlike beta actin, is less metabolically stable.

The variety of peptides derived from the beta actin's N-termini was greater than that of gamma actin. In addition to Met-Asp-Asp-Asp-Ile-Ala-Ala-Leu-(MDDDIAAL-) and Acetyl-Asp-Asp-Asp-Ile-Ala-Ala-Leu-((Ac-DDDIAAL-) N-termini, we also detected the N-terminal peptides sequentially lacking each of the Asp (DDIAAL-, DIAAL-, and IAAL-). Overall, according to intensity estimates, these processed actin species accounted for over ~3% of the total beta actin (Figure 1A, bottom left). No such peptides were detected for gamma actin, which existed solely as a mixture of unprocessed and N-terminally acetylated species (Figure 1A, left).

To test whether similar beta actin processing also occurs in other cell types, we analyzed HAP1 cells, a near-haploid adherent fibroblast-like cell line of human leukemia origin (Carette et al., 2011) commonly used in CRISPR/Cas9 knockout studies. In these cells, no Met containing actin species were detected, suggesting that the removal of N-terminal Met occurs much more rapidly and efficiently than in MEFs. 100% of gamma actin existed as acetylated species (Figure 1A, top right). However, beta actin in these cells also contained a

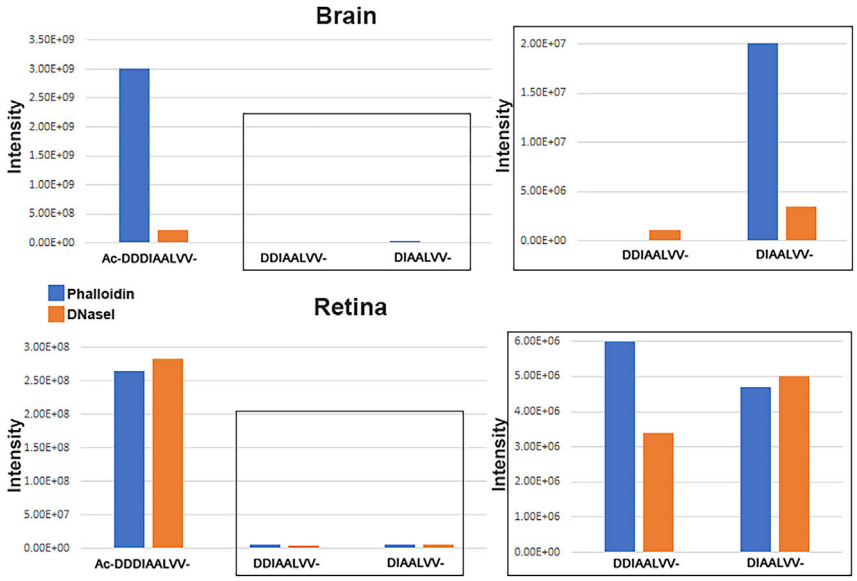

Figure 2. N-terminally processed beta actin incorporates into both F-actin and G-actin pools in vivo

Mass spectrometry detection of the N-terminal beta-actin peptides in biotin-phalloidin and DNaseI agarose pulldowns from brain and retina lysates. Raw intensities from a single experiment are shown for the actin peptides listed on the x axes of the graphs. See Table S2 for the raw intensity values.

smaller but detectable fraction of peptides that had undergone sequential removal of Asp 2, Asp 3, and Asp 4 (Figure 1A, bottom left).

To estimate whether this processing also happens *in vivo*, we tested a purified actin preparation from human platelets, estimated to contain approximately 85% of beta actin and 15% of gamma actin. In this preparation, a ~0.25–0.3% peptide containing one N-terminal D (DIAAL-) was detected, but no other processed peptide species were seen. Notably, according to the intensity ratios performed similarly to those shown in Figure 1A, beta and gamma actin constitutes ~75 and ~25% of this preparation, respectively. This discrepancy from the previously estimated 85%:15% for beta:gamma could be due to the inaccuracy of the intensity measurements, but it may also reflect a potential inaccuracy of the original measurement method. We attempted to evaluate the accuracy of peptide ratio measurements by mixing standard peptides similar to the beta actin N-terminally processed species and performing mass spectrometry on these mixtures, but the results were inconclusive (Dataset 1). Regardless of the origin of this distinction, this measurement provides a reference for our estimations of the percentage of different actin N-terminal peptides in relation to other measurement methods.

N-terminally processed beta actin can be found in both F- and G-actin pool, but is not uniformly present in different tissues *in vivo*

To test whether beta actin processes by N-terminal removal of acidic residues exhibits any preference toward actin monomer or polymer, we performed pulldowns of mouse brain and retina extracts using biotin-phalloidin (that interacts with F-actin) or DNaseI agarose beads (that binds to G-actin). We then tested these pulldowns by mass spectrometry and analyzed the repertoire of N-terminal actin peptides. Remarkably, actin species containing one or two N-terminal D were detected in both pulldowns (Figure 2), suggesting that this processing does happen in these tissues and the processed actins can be found in both F- and G-actin pool. To further estimate their overall abundance in the brain and other tissues, we analyzed actin-sized bands excised from Coomassie-stained gels of whole lysates from the mouse brain, heart, lung, and kidney. None of these tissues contained detectable levels of processed beta actin's N-terminal peptides (Table S2). Since these peptides could be detected in the brain samples after pulldown, we conclude that they are likely still present *in vivo* but at such low levels that they are not easily detectable by mass spectrometry due to the much higher complexity of the whole extract sample compared to the pulldown. This could at least partially be affected by the overall abundance of beta actin in these tissues that also contain major amounts of other actin isoforms.

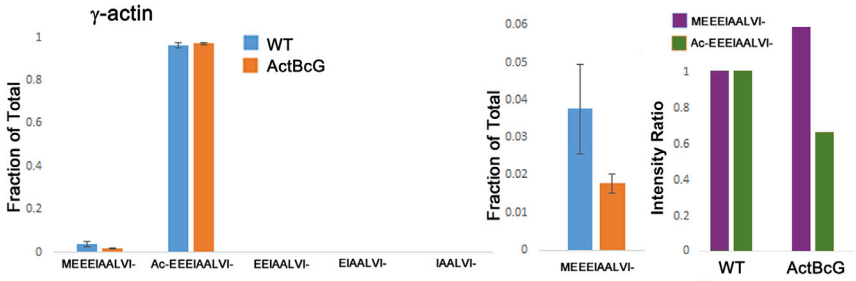

Figure 3. Lack of sequential removal of N-terminal amino acid residues in gamma actin is not nucleotide coding sequence-dependent

Mass spectrometry quantification of the N-terminal gamma-actin peptides in wild type (WT) and gene-edited MEFs expressing gamma actin protein sequence from both beta and gamma actin gene (ActBcG). Left and middle, Ratios of intensities for each peptide versus the total sum of intensities for the entire set of N-terminal peptides are shown on the Y-axis (fraction of the total). N-terminal sequence of each peptide for each isoform is indicated on the X-axis. Error bars represent SEM, n = 3; see Table S4 for the actual values. Right, ratios of average intensities for each peptide across the two samples are shown on the Y-axis, and the corresponding cell genotypes are shown on the X-axis. Intensity ratios are normalized to WT in each run and plotted for each repeat. See Table S2 for the raw intensity values.

Thus, low levels of processed beta actin can be detected *in vivo* as parts of both monomeric and polymeric actin pools.

Lack of N-terminal processing of gamma actin in MEFs is defined by its amino acid sequence

We previously found that beta actin's key functions in cell migration and organism's survival are defined by its nucleotide, rather than amino acid sequence (Vedula et al., 2021). We also found that N-terminal arginylation of beta actin is defined by its nucleotide coding sequence and translation rate (Zhang et al., 2010). To test whether the sequential removal of N-terminal Asp residues in beta actin is nucleotide coding sequence dependent, we used mass spectrometry to analyze MEF in which the endogenous beta actin gene has been edited using CRISPR/Cas9 to encode gamma actin protein, without substantially affecting the nucleotide sequence (beta coded gamma actin or ActBcG (Vedula et al., 2017)). In these cells, gamma actin protein is expressed from both the endogenous beta- and gamma-actin genes. Thus, if the differential N-terminal processing of beta and gamma actin is nucleotide sequence-dependent, N-terminally processed gamma actin with sequentially removed N-terminal Glu should be detected in these cells, unlike in control. However, we found no evidence of such processing (Figure 3). In both wild type and ActBcG cells, the only gamma actin species we detected were either unprocessed, containing N-terminal Met, or acetylated on Glu 2, which constituted the majority of the pool. Curiously, the fraction of Met-uncleaved gamma actin in ActBcG cells was lower than in control, consistent with the observation that beta actin's N-terminal Met removal appears more efficient than gamma actin (Figure 1A, top left). Thus, this difference in Met removal between beta and gamma actin appears to be nucleotide coding sequence dependent. However, further processing of actin by sequential removal of second, third, and fourth negatively charged residues in MEFs is clearly dependent on the amino acid sequence.

Deletion of N-terminal Glu aminopeptidase greatly inhibits sequential removal of N-terminal residues from beta actin *in vivo*

We searched the mouse genome for the candidate enzymes that could perform this processing of the actin's N-termini. The only two aminopeptidases previously shown to possess the activity to remove N-terminal Asp or Glu were Aspartyl and Glutamyl aminopeptidases (DNPEP and ENPEP). Both enzymes are capable of removal of negatively charged residues from the peptide/protein N-termini (Wilk et al., 1998; Yang et al., 2013) and do not appear to strongly discriminate between Asp and Glu. Thus, we used CRISPR/Cas9 to knock out both *DNPEP* and *ENPEP*, individually or together, in HAP1 cells. We then analyzed the effect of these knockouts on the actin N-terminal processing using three independently derived cell lines from each genotype (Figure 4).

Knockout of *DNPEP* did not strongly affect the N-terminal processing of beta actin. In two out of three knockout lines, we did not detect any peptides with DDIAAL- or IAAL- N-terminal sequence, and one

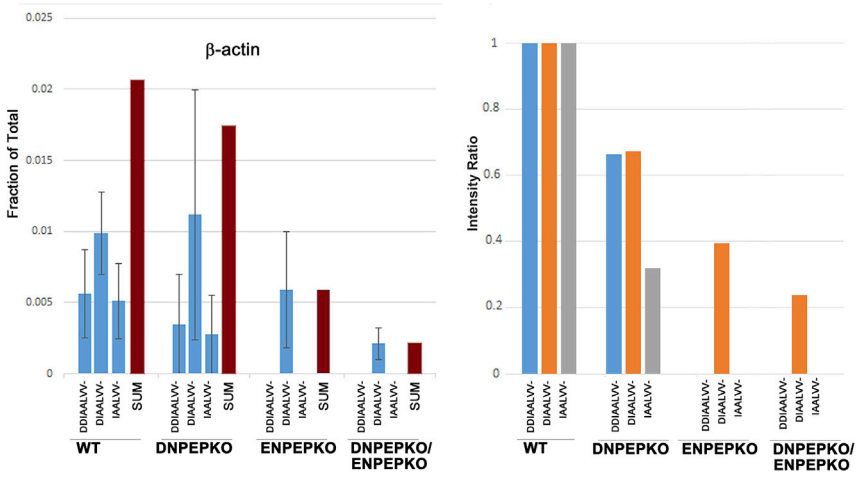

Figure 4. Deletion of Aspartyl and Glutamyl Aminopetidases DNPEP and ENPEP inhibits sequential removal of acidic amino acid residues from beta actin N-terminus

Quantification of N-terminal processing of beta actin from WT, *DNPEP*-KO, *ENPEP*-KO and double knockout HAP1 cells, presented as fraction of the total (left) and as average intensity ratio across samples (right) similarly to that shown in Figure 3. Error bars in the left chart represent SEM, n = 3 independently derived cell lines for each genotype; see Table S4 for the actual values. Individual intensity ratios in the right chart are normalized to WT and plotted for each repeat. See Table S2 for the raw intensity values.

out of three did not contain DIAAL-peptides, however between the three replicates, at least one type of processing was observed in each, suggesting that this knockout might reduce, but not abolish the processing. *ENPEP* knockout had a much stronger effect, with no DDIAAL- or IAAL-peptides detected in any replicate cell lines and the amount of DIAAL-peptide greatly reduced. Double knockout *DNPEP*/*ENPEP* had only trace amount of DIAAL-peptide, and no other peptides from these processing steps detected. Thus, it appears that ENPEP accounts for the majority of the processing, and DNPEP potentially contributes to it, even though it is possible that the DIAAL-peptide can also be generated by some additional enzymatic machinery.

N-terminal Glu aminopeptidase targets non-acetylated actin N-termini and does not differentiate between actin isoforms *in vitro*

Both DNPEP and ENPEP have been characterized as the enzymes that can target N-terminal acidic residues, without an apparent bias toward N-terminal Asp or Glu. With this knowledge, it is unclear how these two enzymes can distinguish between beta and gamma actin, both of which contain a stretch of three acidic residues at the N-terminus. We used *in vitro* assays with synthetic peptides corresponding to the beta and gamma actin's N-terminal sequence to assess whether these enzymes exhibit any specificity toward one of the actin isoforms. In these *in vitro* assays DNPEP did not yield any detectable N-terminally processed peptides, suggesting that this enzyme's activity is low, or actin's N-terminal peptides are not its preferred substrates (Figures S2 and S3). Only ENPEP was able to mediate sequential removal of acidic residues from the peptides' N-termini, with all the processed peptide variants detected after the reaction (Figures S2 and S3). However, this enzyme did not distinguish between beta and gamma actin's N-terminal peptides *in vitro* and processed both with apparently equal efficiency. Thus, if ENPEP accounts for the majority of beta actin's N-terminal processing, as suggested by our *in vivo* data, this enzyme's specificity toward beta rather than gamma actin *in vivo* is likely mediated by additional factors or physiological processes that counteract the action of these enzymes in the context of actin isoforms.

Most of the actin *in vivo* is N-terminally acetylated ((Drazic et al., 2018) and Figure 1). To test whether DNPEP and ENPEP can act on the N-terminally acetylated actin peptides, we performed *in vitro* assays with synthetic peptides containing an acetyl group to mimic the native sequence of beta and gamma actin. In this assay, neither of the enzymes was able to process the acetylated N-terminal Asp of Glu in the beta- or gamma-actin sequence (Figures S4 and S5). This result indirectly suggests that the sequential processing of the actin N-terminal residues by DNPEP and/or ENPEP occurs on non-acetylated actin, likely prior to its targeting by actin N-terminal acetyltransferase NAA80.

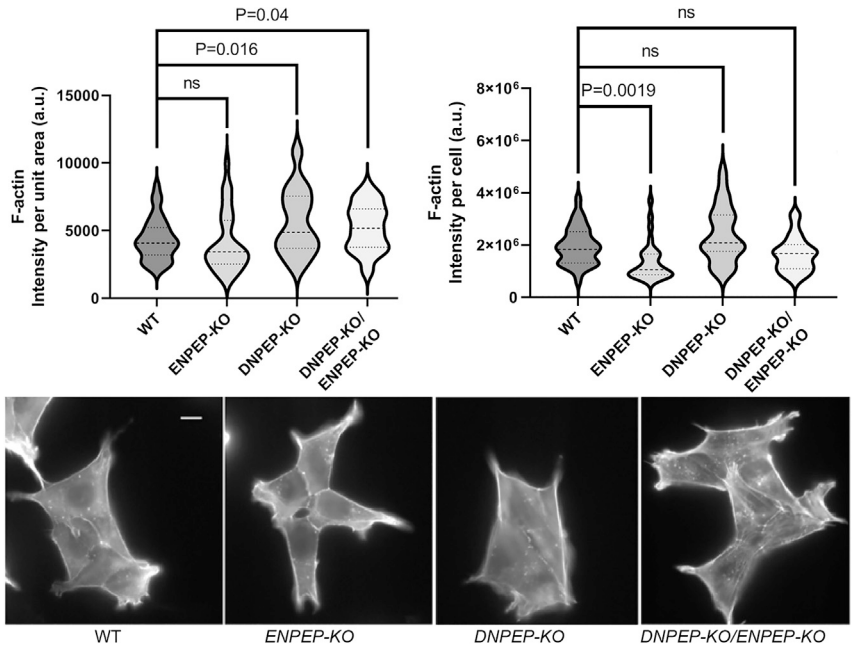

Figure 5. DNPEP and ENPEP knockout results in changes in actin polymer levels in HAP1 cells

Top, violin plots of F-actin per unit area (left) and F-actin per cell (right) detected by Phalloidin-AlexaFluor488 staining of different genotypes; bottom, representative images of different genotypes stained with Phalloidin-AlexaFluor488 (scale bar, 10 μm). n = 31 for WT, 30 for ENPEPKO, 28 for DNPEP KO, and 31 for the double knockout for the intensity per cell measurement, and 31 for WT, 30 for ENPEPKO, 29 for DNPEP KO, and 32 for the double knockout for the intensity per unit area measurement. Data is presented as violin plots with median and quartiles. p values were calculated by unpaired 2-tailed Student's *t* test, ns: $p > 0.05$.

Deletion of N-terminal Asp and Glu aminopeptidase genes affects actin cytoskeleton, filopodia formation, and cell spreading

To test whether DNPEP and ENPEP contribute to actin cytoskeleton-related processes in cells, we analyzed the morphology and basic actin cytoskeleton-dependent processes in *DNPEP* and *ENPEP* knockout HAP1 cells. First, we measured the overall F-actin levels by comparing the average and total staining with fluorescent phalloidin per cell. The unit area intensity was slightly higher in *DNPEP* and *DNPEP/ENPEP* double knockout, suggesting that DNPEP is required for maintaining spatial arrangement of the actin cytoskeleton at the total cell level (Figure 5). This parameter appeared to be unchanged in the *ENPEP* knockout compared to control. In contrast, the total cell intensity of fluorescent phalloidin was significantly lower in *ENPEP* knockout compared to WT, suggesting that this knockout leads to an overall reduction in the amount of polymerized actin per cell. No differences in overall F-actin levels per cell were observed in *DNPEP* knockout cells, and *DNPEP/ENPEP* double knockout showed the same trend as *ENPEP* knockout but with higher p value, possibly because of greater variabilities between replicates in this cell line (Figure 5). Thus, *ENPEP* knockout results in an overall reduction of polymeric actin and *DNPEP* knockout results in potential spatial rearrangement of the actin cytoskeleton.

The number and length of filopodia in both *DNPEP* and *ENPEP* knockout cells was higher than in wild type, and this effect was more pronounced in the double knockout (Figure 6), suggesting that both enzymes contribute to this process in a cumulative manner.

ENPEP knockout, as well as *DNPEP/ENPEP* double knockout, resulted in a significant and pronounced decrease in cell spreading (measured as the area occupied by cells spread on the substrate, Figure 7, left). This effect was not due to a reduction in cell volume, since the size of the spherical trypsinized cells was similar in all cell types (Figure 7, right). Notably, no reduction in cell spreading was observed in *DNPEP* knockout, suggesting that ENPEP is the sole enzyme responsible for this effect.

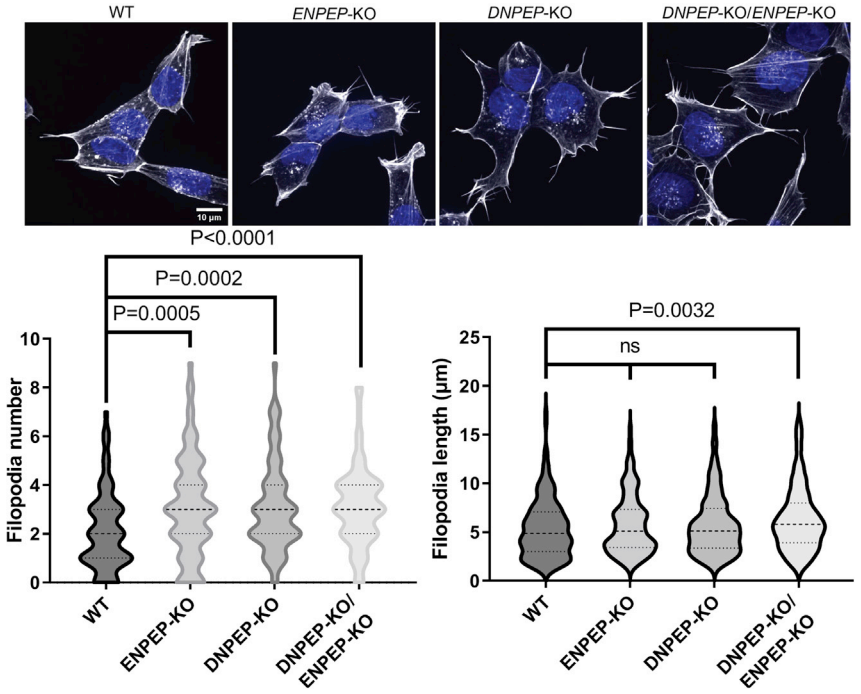

Figure 6. DNPEP and ENPEP knockout results in changes in the number and length of filopodia in HAP1 cells

Top, Representative images of cells from each genotype stained with Phalloidin-AlexaFluor488 (white) and DAPI (blue) (scale bar, 10 µm); bottom, violin plots of filopodia number (left) and length (right). n = 181 for WT, 259 for ENPEPKO, 222 for DNPEP KO, and 205 for the double knockout for the filopodia length measurement, and 84 for WT, 84 for ENPEPKO, 71 for DNPEP KO, and 65 for the double knockout for the filopodia numbers measurement. p values were calculated by unpaired 2-tailed Student's *t* test, ns: $p > 0.05$.

Thus, both DNPEP and ENPEP contribute to actin cytoskeleton maintenance, filopodia formation and cell spreading, and differentially affect these processes, suggesting that they may play different, partially overlapping roles in the actin cytoskeleton maintenance and function.

Deletion of N-terminal Asp and Glu aminopeptidase genes affect cell migration

One of the key functions of non-muscle actin cytoskeleton is its role in cell migration, and it has been previously found that in non-muscle cells beta actin plays a critical role in this process (Perrin and Ervasti, 2010). We therefore compared the rates of migration of HAP1 cells of all four genotypes into an infinite scratch wound in cell culture (Figure 8). *ENPEP* knockout did not substantially affect cell migration rates, but *DNPEP* knockout resulted in substantially slower migration, and this effect was even more pronounced in the double knockout cells. Thus, *DNPEP* critically affects cell migration, even though *ENPEP* potentially also contributes to this process.

DISCUSSION

This study is the first demonstration of previously unknown steps of actin isoform specific N-terminal processing that results in sequential removal of N-terminal Asp residues from beta actin without affecting the closely related gamma actin in the same cells. Actin is one of the striking examples of a protein that possesses a sophisticated enzymatic machinery for multi-step processing of its N-terminus. To date, very few examples of isoform-specific actin processing are known. Our findings add new steps to this processing and further expand the list of isoform-specific actin modifications and potential enzymes involved.

Our data show that while prominent levels of this processing can be detected in cultured cell lines, including immortalized MEFs and HAP1 cells, processed peptides are undetectable in whole mouse tissues, including brain, heart, lungs, and kidney. However, these peptides can be detected in at least some of the enriched actin preparations from native sources, including commercial human platelet actin

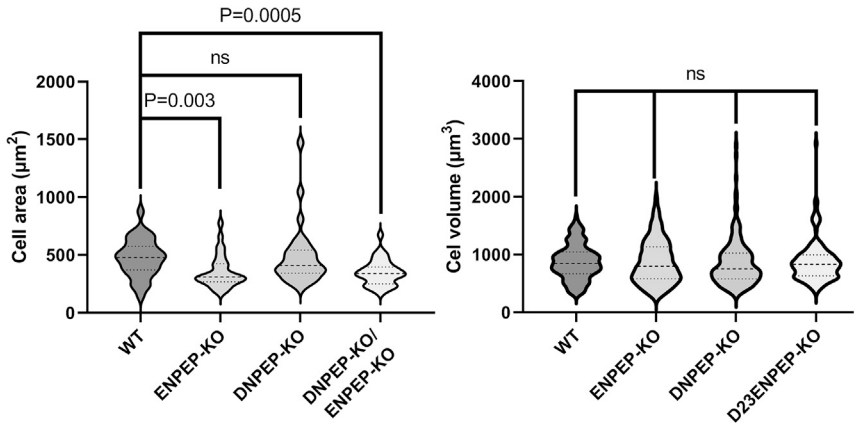

Figure 7. ENPEP knockout results in reduced cell spreading in HAP1 cells

Left, violin plots of the area occupied by spread cells on the substrate; right, violin plots of cell volume, derived from the measurements of trypsinized spherical cells in suspension. Error bars represent SEM, n = 31 for WT, 30 for ENPEPKO, 29 for DNPEP KO, and 32 for the double knockout for the cell area measurement, and 149 for WT, 156 for ENPEPKO, 166 for DNPEP KO, and 139 for the double knockout for the cell volume measurement. p values were calculated by unpaired 2-tailed Student's *t* test, ns: $p > 0.05$.

and brain and retina pulldowns. These results suggest that this processing may be tissue or cell type specific, or overall less prevalent in the whole organisms' environment. It is also possible that, since beta actin in some cases is a minor isoform in these tissues (e.g., heart), 1–3% of its processing is below the detection level of mass spectrometry.

We find that processed beta actin can be found in both F- and G-actin pools after pulldowns from retina and brain extracts. This suggests that processed beta actin is otherwise functional and can incorporate into filaments and undergo disassembly regardless of its N-terminus. An attractive possibility is that processed actin subunits within filaments and/or the monomer pool can affect interactions with actin-binding proteins that are attracted or repelled by the negatively charged actin N-terminal tails exposed on the actin subunit surface (Holmes et al., 1982; Kabsch et al., 1985; Bremer and Aebi, 1992; Chik et al., 1996; Rebowski et al., 2020). Locally applied, such attraction or repulsion can potentially have a profound effect on actin function.

Our results propose two candidate enzymes for mediating N-terminal processing of actin. Aspartyl aminopeptidase (DNPEP) is a cytosolic enzyme that has been largely biochemically characterized, with little insight into its intracellular functions. This enzyme is capable of removing N-terminal Asp or Glu from test substrates structurally similar to synthetic peptides, even though in our *in vitro* assays it did not target the Asp-containing or Glu-containing actin-based peptides, suggesting that this enzyme's activity might be generally low, or that it requires additional cellular cofactors.

ENPEP is largely similar to DNPEP in all these aspects, except that rather than cytosolic, this enzyme is membrane-bound, and it has been previously implicated in regulation of hypertension through the renin-angiotensin system (Yang et al., 2013). ENPEP was initially characterized to have a preference for N-terminal Glu-containing substrates, however our *in vitro* enzymatic assay shows that ENPEP can cleave both Asp and Glu from peptides. In principle, both ENPEP and DNPEP should be able to act on any proteins with exposed N-terminal Asp or Glu. However, very few of such proteins aside from actin are believed to be naturally produced, since the most common class of aminopeptidases known to remove N-terminal Met from newly synthesized proteins, Met-AP1 and Met-AP2, target largely the proteins in which the initiator Met precedes small and uncharged residues (Li and Chang, 1995).

Knockout of DNPEP has a much less pronounced effect on beta actin processing compared to ENPEP knockout. Therefore, it is possible that cellular phenotypes observed in DNPEP knockout cells but not recapitulated in ENPEP knockout may be due to protein targets other than actin. In contrast, the phenotypes common to both knockouts are more likely to arise because of changes in beta actin N-terminal processing.

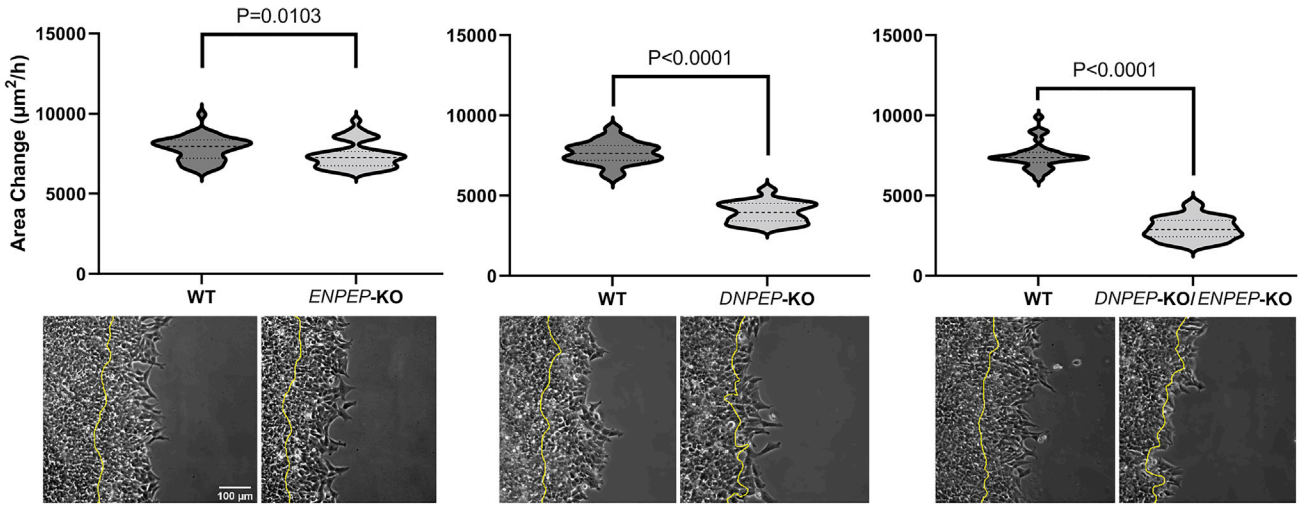

Figure 8. DNPEP knockout affects cell migration in HAP1 cells

Top, violin plots of the cell migration rates in wound healing assays as area covered by the entire wound edge over 12 h of observation, derived as $\mu m^2/h$; bottom, overlay of phase contrast images of the first (0 h) and last (12 h) frame taken from a representative time lapse videos for each genotype. Yellow line in each image outlines the position of the wound edge at 0 time point. Error bars represent SEM, n = 43 for WT and 44 for ENPEPKO in the left chart, 22 for WT and 19 for DNPEP KO in the middle chart, and 37 for WT and 31 for the double knockout in the right chart. p values were calculated by unpaired 2-tailed Student's *t* test.

Human genome encodes 27 proteins with N-terminal MD or ME sequences that can potentially serve as functional DNPEP and ENPEP targets after hypothetical Met- removal, and functions related to actin regulation, actin polymerization and dynamics, and cell adhesion (Figure S7 and Table S3). Knockouts of DNPEP and ENPEP could potentially lead to altered processing and regulation of any of these targets. As an example, some of these proteins are involved in DNA packaging; however, DNPEP and ENPEP knockout cells do not exhibit changes in nuclear size or shape (Figure S8). Actin is a unique protein that possesses a dedicated aminopeptidase to remove its initiator Met to expose a bulky charged residue at the N-terminus (Solomon and Rubenstein, 1985; Chen and Kashina, 2021; MacTaggart and Kashina, 2021). Thus, although we cannot exclude contribution of other protein targets to the effects seen in DNPEP and ENPEP knockout cells, we propose that lack of actin processing is one of the primary reasons for our cellular phenotypes.

It is surprising that gamma actin, unlike beta actin, never undergoes sequential removal of N-terminal acidic residues, given the fact that both beta and gamma actin N-termini are highly homologous and should both fall within the specificity of Asp and Glu aminopeptidases. Moreover, our results show that this preferential ability of beta, but not gamma actin to undergo sequential removal of N-terminal acidic residues is not a property of the beta actin nucleotide sequence, but is amino acid sequence dependent. In combination, these results suggest that the specificity of this processing toward beta actin is likely not defined by the enzymes responsible for the cleavage itself, but rather by a more complex balance of different intracellular pathways mediating different types of intracellular actin processing. Because gamma actin's N-terminus is expected to interact stronger with actin N-terminal acetyltransferase NAA80 due to its stronger negative charge (Rebowski et al., 2020), it is possible that competition with NAA80 may constitute at least one of the mechanisms regulating this N-terminal processing and its selectivity toward beta actin. Notably, removal of Asp residues from beta actin's N-terminus is predicted to reduce or abolish its ability to interact with NAA80. It is likely, however, that the interrelationship between these mechanisms is even more complex.

Removal of Asp 2 from the beta actin sequence exposes the beta actin N-terminus for arginylation, previously shown to target N-terminally exposed Asp 3 (Karakozova et al., 2006) to affect approximately 0.5–0.8% of beta actin at a steady state level in HAP1 cells (Chen and Kashina, 2019). Notably, deletion of *NAA80* increases this fraction by over 10-fold (Vedula et al., 2017). This supports the idea that DNPEP and ENPEP may act as additional enzymes that process unacetylated actin to prime it for arginylation, and possibly other modifications or molecular interactions, before the N-terminal acetylation step. Of note, the beta actin species with a single N-terminal Asp appears to be the most prevalent among the

processed actin variants, and the only one detectable in platelet actin preparations and still present after *ENPEP* knockout. It is possible that a different type of enzyme(s) can remove the Asp-Asp-, Ac-Asp-Asp-, or Met-Asp-Asp di- and tripeptide entities rather than removing single amino acid residues, independently generating this particular actin variant.

Overall, sequential removal of N-terminal beta actin Asp residues targets a very small fraction of intracellular actin, 1–3% or less seen in our studies. Many actin modifications are known to affect a very minor fraction of actin, and it is a topic of extensive debate in the field how such minor modifications can affect the functions of such an abundant protein. One possibility is the existence of localized differentially modified actin pools that arise, e.g., in conjunction with localized *de novo* actin synthesis, in which the percent of modification would be considerably higher. Another possibility is that these effects are amplified via recognition by actin-binding proteins that do not require stoichiometric ratios to cause big changes in actin dynamics. Although at present there are no tools that could address this possibility, it is attractive to suggest that the processing described here constitutes an additional, previously unknown step in actin regulation – e.g., by exposing actin N-terminus to a different class of molecular interactions. This could be especially important in environments where cytoplasmic actins are differentially enriched – e.g., on the leading edge of the cell, or in the nucleus, where beta actin is believed to play a preferential role. These possibilities require further studies.

Actin variants with a reduced or missing stretch of negatively charged amino acids at the N-terminus, even if minor, could greatly expand the variety of functions of this already highly multifunctional protein. The questions of the biological mechanisms that lead form this type of N-terminal actin processing to actin function in cell migration, cytoskeleton maintenance, filopodia protrusion, and other actin-related processes constitute an exciting direction of future studies.

Limitations of the study

Because deletion of DNPEP and ENPEP did not fully abolish the N-terminal processing of beta actin, some of the phenotypic effects seen in the mutants may not be directly related to this processing. Given the broad substrate specificity of DNPEP and ENPEP, this study was unable to fully address the specific effects of beta actin's N-terminal processing by sequential removal of the first few amino acids in cellular functions.

STAR★METHODS

Detailed methods are provided in the online version of this paper and include the following:

- KEY RESOURCES TABLE
- RESOURCE AVAILABILITY
  - Lead contact
  - Materials availability
  - Data and code availability
- EXPERIMENTAL MODEL AND SUBJECT DETAILS
  - Cell culture
  - Vector construction and cell transfection
  - Cell migration assays and imaging
  - Immunofluorescence staining
  - Actin pulldowns with phalloidin and DNaseI agarose
  - Protein and synthetic peptide preparation for mass spectrometry
  - Identification and quantification of N-terminal processing of actin isoforms

SUPPLEMENTAL INFORMATION

Supplemental information can be found online at https://doi.org/10.1016/j.isci.2022.105186.

ACKNOWLEDGMENTS

We thank Thomas Beer from the Wistar Institute Proteomics Facility for the analysis of *in vitro* N-terminally processed peptides and Dr. Yuri I. Wolf from NCBI, NIH for sequence analysis to identify proteins encoding N-terminal MD- and ME-sequences. This work was supported by the NIH grants R35GM122505 and R01NS102435 to AK.

AUTHOR CONTRIBUTIONS

Conceptualization, A.S.K., L.C., and P.V.; Methodology, L.C., P.V., H.Y.T., and D.D.; Investigation, L.C., P.V., D.D., and A.K.; Writing – Original Draft, A.S.K., L.C., and P.V.; Writing – Review & Editing, A.S.K., L.C., P.V., H.Y.T., and D.D.; Funding Acquisition, A.S.K.; Resources, A.S.K. and H.Y.T.; Supervision, A.S.K.

DECLARATION OF INTERESTS

The authors declare no competing interests.

Received: April 8, 2022
Revised: September 2, 2022
Accepted: September 20, 2022
Published: October 21, 2022

REFERENCES

Bremer, A., and Aebi, U. (1992). The structure of the F-actin filament and the actin molecule. Curr. Opin. Cell Biol. *4*, 20–26. https://doi.org/10.1016/0955-0674(92)90054-g.

Bunnell, T.M., Burbach, B.J., Shimizu, Y., and Ervasti, J.M. (2011). beta-Actin specifically controls cell growth, migration, and the G-actin pool. Mol. Biol. Cell *22*, 4047–4058. https://doi.org/10.1091/mbc.E11-06-0582.

Bunnell, T.M., and Ervasti, J.M. (2010). Delayed embryonic development and impaired cell growth and survival in Actg1 null mice. Cytoskeleton (Hoboken) *67*, 564–572. https://doi.org/10.1002/cm.20467.

Bunnell, T.M., and Ervasti, J.M. (2011). Structural and functional properties of the actin gene family. Crit. Rev. Eukaryot. Gene Expr. *21*, 255–266. https://doi.org/10.1615/critreveukargeneexpr.v21.i3.30.

Carette, J.E., Raaben, M., Wong, A.C., Herbert, A.S., Obernosterer, G., Mulherkar, N., Kuehne, A.I., Kranzusch, P.J., Griffin, A.M., Ruthel, G., et al. (2011). Ebola virus entry requires the cholesterol transporter Niemann-Pick C1. Nature *477*, 340–343. https://doi.org/10.1038/nature10348.

Chen, L., and Kashina, A. (2019). Quantification of intracellular N-terminal beta-actin arginylation. Sci. Rep. *9*, 16669. https://doi.org/10.1038/s41598-019-52848-5.

Chen, L., and Kashina, A. (2021). Post-translational modifications of the protein termini. Front. Cell Dev. Biol. *9*, 719590. https://doi.org/10.3389/fcell.2021.719590.

Chik, J.K., Lindberg, U., and Schutt, C.E. (1996). The structure of an open state of beta-actin at 2.65 A resolution. J. Mol. Biol. *263*, 607–623. https://doi.org/10.1006/jmbi.1996.0602.

Cox, J., and Mann, M. (2008). MaxQuant enables high peptide identification rates, individualized p.p.b.-range mass accuracies and proteome-wide protein quantification. Nat. Biotechnol. *26*, 1367–1372. https://doi.org/10.1038/nbt.1511.

Deutsch, E.W., Bandeira, N., Sharma, V., Perez-Riverol, Y., Carver, J.J., Kundu, D.J., García-Seisdedos, D., Jarnuczak, A.F., Hewapathirana, S., Pullman, B.S., et al. (2020). The ProteomeXchange consortium in 2020: enabling 'big data' approaches in proteomics. Nucleic Acids Res. *48*, D1145–D1152. https://doi.org/10.1093/nar/gkz984.

Drazic, A., Aksnes, H., Marie, M., Boczkowska, M., Varland, S., Timmerman, E., Foyn, H., Glomnes, N., Rebowski, G., Impens, F., et al. (2018). NAA80 is actin's N-terminal acetyltransferase and regulates cytoskeleton assembly and cell motility. Proc. Natl. Acad. Sci. USA *115*, 4399–4404. https://doi.org/10.1073/pnas.1718336115.

Fina, M.E., Wang, J., Vedula, P., Tang, H.-Y., Kashina, A., and Dong, D.W. (2022). Arginylation regulates G-protein signaling in the retina. Front. Cell Dev. Biol. *9*, 807345. https://doi.org/10.3389/fcell.2021.807345.

Holmes, K.C., Goody, R.S., and Amos, L.A. (1982). The structure of S1-decorated actin filaments calculated from x-ray diffraction data with phases derived from electron micrographs. Ultramicroscopy *9*, 37–44. https://doi.org/10.1016/0304-3991(82)90227-3.

Kabsch, W., Mannherz, H.G., and Suck, D. (1985). Three-dimensional structure of the complex of actin and DNase I at 4.5 A resolution. EMBO J. *4*, 2113–2118. https://doi.org/10.1002/j.1460-2075.1985.tb03900.x.

Karakozova, M., Kozak, M., Wong, C.C.L., Bailey, A.O., Yates, J.R., 3rd, Mogilner, A., Zebroski, H., and Kashina, A. (2006). Arginylation of beta-actin regulates actin cytoskeleton and cell motility. Science *313*, 192–196. https://doi.org/10.1126/science.1129344.

Li, X., and Chang, Y.H. (1995). Amino-terminal protein processing in Saccharomyces cerevisiae is an essential function that requires two distinct methionine aminopeptidases. Proc. Natl. Acad. Sci. USA *92*, 12357–12361. https://doi.org/10.1073/pnas.92.26.12357.

MacTaggart, B., and Kashina, A. (2021). Posttranslational modifications of the cytoskeleton. Cytoskeleton (Hoboken) *78*, 142–173. https://doi.org/10.1002/cm.21679.

Perez-Riverol, Y., Bai, J., Bandla, C., García-Seisdedos, D., Hewapathirana, S., Kamatchinathan, S., Kundu, D.J., Prakash, A., Frericks-Zipper, A., Eisenacher, M., et al. (2022). The PRIDE database resources in 2022: a hub for mass spectrometry-based proteomics evidences. Nucleic Acids Res. *50*, D543–D552. https://doi.org/10.1093/nar/gkab1038.

Perrin, B.J., and Ervasti, J.M. (2010). The actin gene family: function follows isoform. Cytoskeleton (Hoboken) *67*, 630–634. https://doi.org/10.1002/cm.20475.

Rebowski, G., Boczkowska, M., Drazic, A., Ree, R., Goris, M., Arnesen, T., and Dominguez, R. (2020). Mechanism of actin N-terminal acetylation. Sci. Adv. *6*, eaay8793. https://doi.org/10.1126/sciadv.aay8793.

Rubenstein, P.A., and Martin, D.J. (1983). NH2-terminal processing of actin in mouse L-cells in vivo. J. Biol. Chem. *258*, 3961–3966. http://www.ncbi.nlm.nih.gov/pubmed/6833238.

Sakuma, T., Nishikawa, A., Kume, S., Chayama, K., and Yamamoto, T. (2014). Multiplex genome engineering in human cells using all-in-one CRISPR/Cas9 vector system. Sci. Rep. *4*, 5400. https://doi.org/10.1038/Srep05400.

Sheff, D.R., and Rubenstein, P.A. (1992). Isolation and characterization of the rat liver actin N-acetylaminopeptidase. J. Biol. Chem. *267*, 20217–20224. http://www.ncbi.nlm.nih.gov/pubmed/1400339.

Solomon, L.R., and Rubenstein, P.A. (1985). Correct NH2-terminal processing of cardiac muscle alpha-isoactin (class II) in a nonmuscle mouse cell. J. Biol. Chem. *260*, 7659–7664. http://www.ncbi.nlm.nih.gov/pubmed/3997892.

Terman, J.R., and Kashina, A. (2013). Post-translational modification and regulation of actin. Curr. Opin. Cell Biol. *25*, 30–38. https://doi.org/10.1016/j.ceb.2012.10.009.

Vandekerckhove, J., and Weber, K. (1978a). Actin amino-acid sequences. Comparison of actins from calf thymus, bovine brain, and SV40-transformed mouse 3T3 cells with rabbit skeletal muscle actin. Eur. J. Biochem. *90*, 451–462. https://doi.org/10.1111/j.1432-1033.1978.tb12624.x.

Vandekerckhove, J., and Weber, K. (1978b). At least six different actins are expressed in a higher mammal: an analysis based on the amino acid sequence of the amino-terminal tryptic peptide. J. Mol. Biol. *126*, 783–802. https://doi.org/10.1016/0022-2836(78)90020-7.

Vandekerckhove, J., and Weber, K. (1978c). Comparison of the amino acid sequences of three tissue-specific cytoplasmic actins with

rabbit skeletal muscle actin [proceedings]. Arch. Int. Physiol. Biochim. *86*, 891–892. http://www.ncbi.nlm.nih.gov/pubmed/84600.

Vandekerckhove, J., and Weber, K. (1978d). Mammalian cytoplasmic actins are the products of at least two genes and differ in primary structure in at least 25 identified positions from skeletal muscle actins. Proc. Natl. Acad. Sci. USA *75*, 1106–1110. https://doi.org/10.1073/pnas.75.3.1106.

Vedula, P., and Kashina, A. (2018). The makings of the 'actin code': regulation of actin's biological function at the amino acid and nucleotide level. J. Cell Sci. *131*, jcs215509. https://doi.org/10.1242/jcs.215509.

Vedula, P., Kurosaka, S., Leu, N.A., Wolf, Y.I., Shabalina, S.A., Wang, J., Sterling, S., Dong, D.W., and Kashina, A. (2017). Diverse functions of homologous actin isoforms are defined by their nucleotide, rather than their amino acid sequence. Elife *6*, e31661. https://doi.org/10.7554/eLife.31661.

Vedula, P., Kurosaka, S., MacTaggart, B., Ni, Q., Papoian, G., Jiang, Y., Dong, D.W., and Kashina, A. (2021). Different translation dynamics of beta- and gamma-actin regulates cell migration. Elife *10*, e68712. https://doi.org/10.7554/eLife.68712.

Wilk, S., Wilk, E., and Magnusson, R.P. (1998). Purification, characterization, and cloning of a cytosolic aspartyl aminopeptidase. J. Biol. Chem. *273*, 15961–15970. https://doi.org/10.1074/jbc.273.26.15961.

Yang, Y., Liu, C., Lin, Y.L., and Li, F. (2013). Structural insights into central hypertension regulation by human aminopeptidase A. J. Biol. Chem. *288*, 25638–25645. https://doi.org/10.1074/jbc.M113.494955.

Zhang, F., Saha, S., Shabalina, S.A., and Kashina, A. (2010). Differential arginylation of actin isoforms is regulated by coding sequence-dependent degradation. Science *329*, 1534–1537. https://doi.org/10.1126/science.1191701.

STAR★METHODS

KEY RESOURCES TABLE

REAGENT AND RESOURCE	SOURCE	IDENTIFIER
Iscove's Modified Dulbecco's Medium	Thermo Fisher Scientific, USA	Cat #: 31980030
Eagle's minimal essential medium	Thermo Fisher Scientific, USA	Cat #: 10569010
Fetal Bovine Serum	Sigma-Aldrich, USA	Cat #: F2442-500ML
penicillin/streptomycin	Corning, USA	Cat #: 30-002-CI
FuGENE 6	Promega, USA	Cat #: E5911
Trypsin	Invitrogen, USA	Cat #: 15400054
Paraformaldehyde aqueous solution	Electron Microscopy Sciences, USA	Cat #: 15710
Phalloidin conjugated to AlexaFluor 594	Thermo Fisher Scientific, USA	Cat #: A12381
DAPI	Thermo Fisher Scientific, USA	Cat #: 62248
Protease inhibitors cocktail	Sigma, USA	Cat #: P8340
HEPES	Fisher Scientific, CA	Cat #: BP310-100
NaCl	Fisher Scientific, CA	Cat #: S271-500
$MgCl_2$	Fisher Scientific, CA	Cat #: 600-30-96
ATP	Sigma, USA	Cat #: A2383-1G
DNaseI	Sigma, USA	Cat #: 11284932001
SDS	Bio-Rad, USA	Cat #: 1610302
Coomassie blue R-250	Bio-Rad, USA	Cat #: 1610400
Human platelet actin	Cytoskeleton, USA	Cat #: APHL99-A
Tris(2-carboxyethyl) phosphine	Thermo Fisher Scientific, USA	Cat #: 040587.09
Iodoacetamide	Thermo Fisher Scientific, USA	Cat #: 122270050
Synthetic peptides	GenScript, USA	N/A
DNPEP	OriGene, USA	Cat#: TP300104
ENPEP	Novus Biologicals, USA	Cat#: 2499-ZN-010
$CaCl_2$	Fisher Scientific, CA	Cat#: MP21995245
Acetonitrile	Fisher Scientific, CA	Cat#: AA22927M1
Trifluoroacetic acid	Sigma, USA	Cat#: 302031-100ML
Multiplex CRISPR/Cas9 Assembly System Kit	Addgene, USA	Cat#: 1000000055
MaxQuant 1.6.17.0	Max-Planck Institute for Biochemistry	https://www.maxquant.org/
Xcalibur software	Thermo Fisher Scientific, USA	Cat#: OPTON-30965
ImageJ	NIH	https://imagej.nih.gov/ij/
Proteomics datasets	ProteomeXchange Consortium	PXD031462, PXD031465, PXD031481, PXD032086, PXD032139

RESOURCE AVAILABILITY

Lead contact

Anna S. Kashina, akashina@upenn.edu.

Materials availability

All materials generated in this work are available upon request from the lead contact.

Data and code availability

- Data: The mass spectrometry proteomics data have been deposited to the ProteomeXchange Consortium (Deutsch et al., 2020) via the PRIDE (Perez-Riverol et al., 2022) partner repository with the dataset identifiers PXD031462, PXD031465, PXD031481, PXD032086, and PXD032139.
- Code: N/A
- All other items: N/A

EXPERIMENTAL MODEL AND SUBJECT DETAILS

Human HAP1 cells were obtained from ATCC and used to produce the D*NPEP*-KO, *ENPEP*-KO and *DNPEP*/*ENPEP*-KO cell lines as described in this paper.

Immortalized wild type mouse embryonic fibroblasts (MEF) were obtained in the lab from E12.5 mouse embryos (*Mus musculus*) and immortalized by continuous passaging in culture as described in (Karakozova et al., 2006). Animal gender was not determined for the cell isolation. Actin-edited MEFs and tissues were isolated from actin-edited mice and immortalized in culture as described in (Vedula et al., 2017). All animal work during cell and tissue derivation was performed in compliance with the University of Pennsylvania Institutional Animal Care and Use Committee (IACUC) guidelines, under IACUC-approved protocols.

Cell culture

Wildtype and knockout HAP1 cells were cultured as described by (Drazic, A. et al.). MEFs were cultured in DMEM (high glucose with GlutaMAX, Gibco Life Technology) containing 10% fetal bovine serum and 1% Penicillin-Streptomycin (Antibiotic-Antimycotic solution; Life Technology) at 37°C with 5% CO_2. Cells were routinely checked for contamination.

Vector construction and cell transfection

To generate related gene knockout cells, CRISPR/Csa9 all-in-one expression vectors containing multiple guide RNA expression cassettes and a Cas9 nickase cassette were used for targeted gene deletion (deletion scheme and results were showed in Figure S6). Detailed procedures were described by Sakuma et al. (2014), and the oligos for vector construction and knockout cell genotyping were listed in Table S1. HAP1 cells were cultivated in Iscove's Modified Dulbecco's Medium (IMDM) with the addition of 10% FBS and 1% penicillin/streptomycin. Briefly 70–90% confluent cells in 6-well plated were transfected with 1 μg CRISPR/Cas9 plasmids per well by using FuGENE 6 (Promega, Madison, WI). After 24 h after transfection, 2 μg/mL puromycin were added to the cell culture and incubated for 48 h followed by splitting cells into 96-well plates to reach 0.5 cell per well.

Cell migration assays and imaging

Cells were grown to a confluent monolayer, and half of this monolayer was scraped off the dish with a sharp razor blade to enable continuous directional migration into the empty area of the dish for ~12 h of observation. Cells monolayer after scratching was incubated for 2 h before imaging to enable recovery of cells at the wound edge. Migration rates were measured as the area covered by the edge of the wound in the field of view per unit time using Fiji. Images were acquired by a Nikon Ti microscope with 20X Phase objective and Andor iXon Ultra 888 EMCCD camera.

Immunofluorescence staining

To quantitate the amount of F-actin, spreading area, filopodia, and nuclei, HAP1 cell culture with 70–80% confluence were trypsinized and diluted 4-fold followed by seeded on coverslips in 6-well plates. The cells were cultivated for 24 h and then fixed in 4% paraformaldehyde aqueous solution (PFA) at room temperature for 30 min followed by washing with PBS three times. Cells were then stained with Phalloidin conjugated to Alexa Fluor 594 (Molecular Probes, Eugene, OR) and DAPI (Thermo Fisher Scientific, Waltham, MA). Cell images were acquired by using Nikon Ti microscope with 100X objective and Andor iXon Ultra 888 EMCCD camera. Cell filopodia were imaged by Nikon Ti microscope with 100X objective lens, equipped with a spinning disk CSU-22 (Yokogawa) and Andor iXon Life IXON-L-897 EMCCD camera. All images were analyzed by fiji (NIH, Bethesda, MD).

For measurements of F-actin per cell, isolated islands of HAP1 cells were thresholded against the background and F-actin levels were measured as total gray levels in the island divided by the number of nuclei seen in the DAPI channel.

Actin pulldowns with phalloidin and DNaseI agarose

Freshly excised brain and retina tissue was flash frozen in LN2 and homogenized by grinding in LN2 with mortar and pestle. The powder was transferred into pre-chilled tube on ice and mixed with ice-cold lysis buffer (100mM HEPES pH 7.4, 50mM NaCl, 2mM $MgCl_2$, 2mM ATP, and protease inhibitors cocktail (Sigma)) and passed through a 21½ G syringe on ice. The lysate was clarified at 6,000 g, 10 min, 4°C, mixed with Phalloidin-Biotin (for F-actin) or DNaseI agarose (for G-actin), and incubated on a rocker for 2 h at 4°C. Pulldowns were collected by addition of magnetic streptavidin beads (for Phalloidin), or centrifugation (for DNaseI agarose), washed 3 times with lysis buffer, eluted into SDS sample buffer, and fractionated by a short run on SDS PAGE. The entire protein zone after Coomassie blue staining was excised and processed by in-gel digestion as mass spectrometry.

Protein and synthetic peptide preparation for mass spectrometry

HAP1 and MEF cells with 70–80% confluence were harvested by scraping and centrifugation. The pellets were washed by PBS, and spun down to remove the supernatant. The cell pellets were lysed directly in 4 × SDS sample buffer at the W:V ratio of 1: 10 (1 mg cell: 10 μL buffer), followed by boiling in water for 10 min 10 μL of each sample was loaded for SDS-PAGE electrophoresis at 150 V. Human platelet actin was purchased from Cytoskeleton, Inc. (Cat. #APHL99-A), and aliquotes were dissolved in SDS sample buffer and run on SDS-PAGE electrophoresis. The actin bands were excised from the gel, reduced with tris(2-carboxyethyl)phosphine, alkylated with iodoacetamide, and digested with trypsin. The trypsin digested actin was analyzed using a standard 90-min LC gradient on the Thermo Q Exactive Plus mass spectrometer. The mass spectrometry data were searched with partial tryptic specificity against the mammalian actin isoform database and a contaminant database using MaxQuant 1.6.17.0.

The synthetic peptides (Ac-DDDIAALC, Ac-EEEIAALC, DDDIAALC, EEEIAALC) were synthesized by GenScript (Piscataway, NJ). The DNPEP and ENPEP proteins were purchased from OriGene (Cat#: TP300104) and Novus Biologicals (Cat#: 2499-ZN-010) respectively. The enzymatic assay was modified from ENPEP assay procedures: 200 μL reaction system (25 mM Tris, 50 mM CaCl2, 0.2 M NaCl, pH 8.0) containing 100 μM peptide and 400 ng recombinant proteins were incubated at 37°C for 30 min, then terminate the reactions by heating at 95°C for 15 min followed by keeping the tubes on ice for 20 min. Spin the tube at 17,000 x g for 15minat RT and load the supernatants onto C18 spin columns prewashed with 100% acetonitrile and water by centrifugation at 110 x g for 1 min. Wash the columns with 150 μL peptide wash buffer (0.1% trifluoroacetic acid (TFA) in water) two times followed by eluting the column-bound peptides with 150 μL of peptide elution buffer two times. The elutes were gone through SpeedVac vacuum concentrators to reduce the volume to 10–20 μL. 5 μL of 20 mM TCEP was added to 10 μL of Sample and incubated for 20–30 min at 37°C, then the sample were analyzed by Q Exactive HF Mass Spec. Data were analyzed by Xcalibur software.

Identification and quantification of N-terminal processing of actin isoforms

Data analysis was performed on the samples processed as.raw files using MaxQuant software (Cox and Mann, 2008) as described in (Fina et al., 2022). To avoid mis-assignment of processed peptides, we did two complete search runs for each raw data file. The first run was against the mouse or human protein database and a locally compiled list of contaminants, using static carboxamidomethylation of Cys, and variable Met oxidation, protein N-terminal acetylation, and Asn deamidation. In the second run, the "MS/MS first search" (used for mass recalibration in MaxQuant) was the same as the first run, but the "MS/MS main search" and the "Second peptide search" were against a limited fasta file containing only the mammalian actin sequences, and including arginylation, monomethylarginylation, and dimethylarginylation on any D and E as a variable modification. In addition, "Match between runs" and "Dependent peptides" options were enabled in the second run. Consensus identification lists were generated with false discovery rates of 1% at the protein, peptide and modification site levels. We excluded the processed peptides identified in the second run if they were from the scans which have at least one peptide identified in the first run with a different sequence.

For quantification of the actin N-terminal peptides, all the peptides corresponding to the beta and gamma actin N-termini were separated out and divided into groups according to their N-terminal residue (Met1, acetylated Asp/Glu2, Asp/Glu3, Asp/Glu4, or Ile/Val5), regardless of any additional variable modifications. Of note, no N-terminal acetylation on Met or the residues past the Asp/Glu2 were detected. Intensities of each peptide species were added together and divided by the total intensity added for the entire repertoire of the N-termini for each actin isoform to obtain fractions of the total shown in the figures.